CURVE EVOLUTION, BOUNDARY-VALUE STOCHASTIC PROCESSES, THE MUMFORD-SHAH PROBLEM, AND MISSING DATA APPLICATIONS

Andy Tsai[†] *Anthony Yezzi, Jr.*[‡] *Alan S. Willsky*[†]

[†] Department of Electrical Engineering
and Computer Science
Massachusetts Institute of Technology
Cambridge, MA 02139

[‡] School of Electrical and Computer
Engineering
Georgia Institute of Technology
Atlanta, GA 30332

ABSTRACT

We present an estimation-theoretic approach to curve evolution for the Mumford-Shah problem. By viewing an active contour as the set of discontinuities in the Mumford-Shah problem, we may use the corresponding functional to determine gradient descent evolution equations to deform the active contour. In each gradient descent step, we solve a corresponding optimal estimation problem, connecting the Mumford-Shah functional and curve evolution with the theory of boundary-value stochastic processes. In employing the Mumford-Shah functional, our active contour model inherits its attractive ability to generate, in a coupled manner, both a smooth reconstruction and a segmentation of the image.

Next, by generalizing the data fidelity term of the original Mumford-Shah functional to incorporate a spatially varying penalty, we extend our method to problems in which data quality varies across the image and to images in which sets of pixel measurements are missing. This more general model leads us to a novel PDE-based approach for simultaneous image magnification, segmentation, and smoothing, thereby extending the traditional applications of the Mumford-Shah functional which only considers simultaneous segmentation and smoothing.

1. INTRODUCTION

A novel active contour model is introduced in this paper for the Mumford-Shah problem of simultaneous image smoothing and segmentation. In particular, by constraining the set of discontinuities in the Mumford-Shah problem to correspond to an evolving set of curves, we derive the gradient descent curve evolution that seeks the local minimum of the Mumford-Shah functional. Each gradient descent step involves solving a corresponding optimal estimation problem, namely the estimation of the noise-free image given the noisy image data and the current estimate of the boundary curve. The solution of this estimation problem comes from the theory of boundary-value stochastic processes, which leads to decoupled partial differential equations (PDE's) in space whose solutions produce the optimal image estimates in each of the connected regions separated by the current curve estimate. This theory also gives us boundary conditions for these estimates along the current estimate of the boundary curve which are directly used in evolving the curve.

This work was supported by ONR grant N00014-91-J-1004 and by subcontract GC123919NGD from Boston University under the AFOSR Multidisciplinary Research Program.

This active contour model can be considered as a curve evolution driven by solutions of a continuum of auxiliary spatial estimation problems. Our work may be regarded as an extension of several recent region based approaches to curve evolution [2, 5, 7]. In particular, this work naturally generalizes the very nice work of Chan and Vese who consider curve evolution methods based upon piece-wise constant variants of the Mumford-Shah functional in [2] and who have independently and contemporaneously developed ideas very similar to those presented in this paper.[1]

The active contour model inherits the attractive ability of the Mumford-Shah technique to generate, in a coupled manner, a segmentation and a smooth reconstruction of the image. Our model can also automatically segment images with multiple region types (perhaps each with different mean intensities) without knowing a priori how many distinct regions are present in the image.

In the next part of this paper, we introduce a spatially varying penalty into the data fidelity term, allowing us to treat images in which the quality of the measurements vary depending upon pixel location. In particular, we are able to treat, as a limiting case, images containing sets of pixels without measurements. By applying this missing data technique in a structured manner, we are able to develop a novel, unified framework for image magnification, segmentation, and smoothing. This technique constitutes a more global approach to magnification when compared to more traditional bilinear or bicubic interpolation schemes, while still maintaining sharp transitions along region boundaries. Furthermore, the arclength penalty prevents the appearance of blocky object boundaries that arise in replication-based schemes.

2. AN ESTIMATION-THEORETIC APPROACH TO CURVE EVOLUTION FOR THE MUMFORD-SHAH PROBLEM

The point of reference for this paper is the Mumford-Shah functional

$$E(\mathbf{f},\vec{C})=\beta\iint_{\Omega}(\mathbf{f}-\mathbf{g})^2\ dA+\alpha\iint_{\Omega\setminus\vec{C}}|\nabla\mathbf{f}|^2\ dA\ +\gamma\oint_{\vec{C}}ds \quad (1)$$

in which $\mathbf{g}$ denotes the data, $\mathbf{f}$ denotes a piecewise-smooth approximation of $\mathbf{g}$, $\vec{C}$ denotes a smooth segmenting curve, and Ω denotes the image domain [3]. The parameters α, β, and γ control

[1] Chan and Vese recently posted a technical report in which they generalize their previous approach (see www.math.ucla.edu/applied/cam/).

0-7803-6297-7/00/$10.00 © 2000 IEEE

the competition between the various terms above. The Mumford-Shah problem is to minimize $E(\mathbf{f}, \vec{C})$ over admissible $\mathbf{f}$ and $\vec{C}$. We now present how this problem is solved via a curve-evolution-based approach.

2.1. Optimal image estimation and boundary-value stochastic processes

For any arbitrary closed curve $\vec{C}$ in the image domain, Ω is partitioned into R and R^c, corresponding to the image domain inside and outside the curve, respectively. Given such a $\vec{C}$, we wish to find estimates of $\mathbf{f}_R$ and $\mathbf{f}_{R^c}$, the $\mathbf{f}$ in regions R and R^c respectively, that minimizes

$$E_{\vec{C}}(\mathbf{f}_R, \mathbf{f}_{R^c}) = \beta \iint\limits_R (\mathbf{f}_R - \mathbf{g})^2\, dA + \alpha \iint\limits_R |\nabla \mathbf{f}_R|^2\, dA + \beta \iint\limits_{R^c} (\mathbf{f}_{R^c} - \mathbf{g})^2\, dA + \alpha \iint\limits_{R^c} |\nabla \mathbf{f}_{R^c}|^2\, dA. \quad (2)$$

The estimate $\hat{\mathbf{f}}_R$ that minimizes (2) is also the solution to finding the estimate of a boundary-value stochastic process $\mathbf{f}_R$ on the domain R whose measurement equation is

$$\mathbf{g} = \mathbf{f}_R + \mathbf{v}$$

and whose prior probabilistic model is given by

$$\nabla \mathbf{f}_R = \mathbf{w}$$

where $\mathbf{v}$ and $\mathbf{w}$ are independent white Gaussian random vectors with covariances $\frac{1}{\beta}\mathbf{I}$ and $\frac{1}{\alpha}\mathbf{I}$, respectively. The linear estimation of this boundary-value stochastic process can be solved by the method of complementary models [1]. Using this method, we derive $\hat{\mathbf{f}}_R$ as the solution to the following:

$$\begin{aligned} \hat{\mathbf{f}}_R - \frac{\alpha}{\beta}\nabla^2 \hat{\mathbf{f}}_R &= \mathbf{g} \qquad \text{on } R \\ \frac{\partial \hat{\mathbf{f}}_R}{\partial \vec{\mathcal{N}}} &= 0 \qquad \text{on } \vec{C} \end{aligned}$$

where $\vec{\mathcal{N}}$ denotes the outward unit normal of the curve $\vec{C}$. In a similar fashion, we derive $\hat{\mathbf{f}}_{R^c}$ as the solution to the following:

$$\begin{aligned} \hat{\mathbf{f}}_{R^c} - \frac{\alpha}{\beta}\nabla^2 \hat{\mathbf{f}}_{R^c} &= \mathbf{g} \qquad \text{on } R^c \\ \frac{\partial \hat{\mathbf{f}}_{R^c}}{\partial \vec{\mathcal{N}}} &= 0 \qquad \text{on } \vec{C}. \end{aligned}$$

Conjugate gradients (CG) method is used to solve the above PDE's.

2.2. Gradient descent equation of the Mumford-Shah functional

With the ability to calculate $\hat{\mathbf{f}}_R$ and $\hat{\mathbf{f}}_{R^c}$ for any given $\vec{C}$, we now wish to derive a curve evolution for $\vec{C}$ that minimizes (1). That is, as a function of $\vec{C}$, we wish to find $\vec{C}_t$ that minimizes

$$\begin{aligned} E_{\hat{\mathbf{f}}_R, \hat{\mathbf{f}}_{R^c}}(\vec{C}) = {} & \beta \iint\limits_R (\hat{\mathbf{f}}_R - \mathbf{g})^2\, dA + \alpha \iint\limits_R |\nabla \hat{\mathbf{f}}_R|^2\, dA \\ & + \beta \iint\limits_{R^c} (\hat{\mathbf{f}}_{R^c} - \mathbf{g})^2\, dA + \alpha \iint\limits_{R^c} |\nabla \hat{\mathbf{f}}_{R^c}|^2\, dA \\ & + \gamma \oint\limits_{\vec{C}} ds. \end{aligned} \quad (3)$$

The curve evolution that minimizes (3) is derived as

$$\begin{aligned} \vec{C}_t = {} & \frac{\alpha}{2}\left(|\nabla \hat{\mathbf{f}}_{R^c}|^2 - |\nabla \hat{\mathbf{f}}_R|^2\right)\vec{\mathcal{N}} \\ & + \frac{\beta}{2}\left((\mathbf{g} - \hat{\mathbf{f}}_{R^c})^2 - (\mathbf{g} - \hat{\mathbf{f}}_R)^2\right)\vec{\mathcal{N}} - \gamma\kappa\vec{\mathcal{N}} \end{aligned}$$

where κ denotes the signed curvature of $\vec{C}$. This flow is implemented via the level set method [4].

3. IMPLEMENTATION

The algorithm described in the previous section requires solving two PDE's at every evolution step of the curve making it computationally expensive and impractical. We propose an approximate gradient descent approach to calculate $\hat{\mathbf{f}}_R$, $\hat{\mathbf{f}}_{R^c}$, and $\vec{C}$ to alleviate some of the computational burdens. This approach consists of alternating between these two steps:

- Fix $\hat{\mathbf{f}}_R$ and $\hat{\mathbf{f}}_{R^c}$, and take several gradient descent curve evolution steps to move the curve $\vec{C}$.
- Fix $\vec{C}$, and perform just a few iterations of the CG procedure–without taking it to convergence–to obtain a *rough* estimate of $\mathbf{f}_R$ and $\mathbf{f}_{R^c}$.

Only a rough estimate of $\mathbf{f}_R$ and $\mathbf{f}_{R^c}$ is required to direct the curve to move in the descent direction. The idea is to make the algorithm faster by reducing the number of times $\hat{\mathbf{f}}_R$ and $\hat{\mathbf{f}}_{R^c}$ are calculated and also the amount of time required to calculate each of them. CG procedure is carried to convergence in the last iteration to obtain an accurate estimate of $\mathbf{f}_R$ and $\mathbf{f}_{R^c}$.

Figure 1 illustrates the performance of this implementation of our model by using a noisy image of two Star Wars characters standing in a spatially varying background. The segmentation clearly delineated the two Star Wars characters. The reconstruction of the image accurately captured the spatially varying background and preserved the structures within each Star Wars character. Obviously, this is not possible with lower dimensional models.

4. MISSING DATA APPLICATIONS

So far, we have focused on developing our algorithm for the particular context in which the Mumford-Shah functional was originally designed, namely simultaneous image segmentation and denoising. However, the range of applications of our algorithm is much richer. In this section, we extend the approach of previous section to solve missing data problems by generalizing the original Mumford-Shah functional.

4.1. Segmentation, denoising, and interpolation of images with missing data

Our model handles missing data through the parameter β. In the standard Mumford-Shah formulation (1), β is a constant scalar parameter reflecting our confidence in the measurements. To accommodate applications in which the data quality is spatially varying and even in the limiting such case in which there are missing pixel measurements distributed arbitrarily through the image domain, we replace the constant parameter β by a spatially varying function $\boldsymbol{\beta}$ whose value at each pixel is inversely proportional to the variance of the measured noise at that pixel. For example, in the situation where the data at pixel (x_o, y_o) is missing, we consider

(a) (b) (c) (d) (e)

Fig. 1. *Noisy image of Star Wars characters Qui-Gon Jinn and Jar Jar Binks in the Tatooine Desert.*

the variance of the data at that pixel as being infinite and accordingly set $\beta(x_o, y_o) = 0$. By introducing this spatially varying β, equation (1) becomes:

$$E(\mathbf{f}, \vec{C}) = \iint_{\Omega} \beta(\mathbf{f} - \mathbf{g})^2 \, dA + \alpha \iint_{\Omega \setminus \vec{C}} |\nabla \mathbf{f}|^2 \, dA + \gamma \oint_{\vec{C}} ds. \quad (4)$$

The gradient flow that minimizes (4) is given by

$$\begin{aligned} \vec{C}_t &= \frac{\alpha}{2}\left(|\nabla \hat{\mathbf{f}}_{R^c}|^2 - |\nabla \hat{\mathbf{f}}_R|^2\right)\vec{\mathcal{N}} \\ &+ \frac{\beta}{2}\left((\mathbf{g} - \hat{\mathbf{f}}_{R^c})^2 - (\mathbf{g} - \hat{\mathbf{f}}_R)^2\right)\vec{\mathcal{N}} - \gamma\kappa\vec{\mathcal{N}} \quad (5) \end{aligned}$$

where the optimal estimates $\hat{\mathbf{f}}_R$ and $\hat{\mathbf{f}}_{R^c}$ of (5) satisfy

$$\begin{aligned} \beta\hat{\mathbf{f}}_R - \alpha\nabla^2\hat{\mathbf{f}}_R &= \beta\mathbf{g} && \text{on } R \\ \frac{\partial \hat{\mathbf{f}}_R}{\partial \vec{\mathcal{N}}} &= 0 && \text{on } \vec{C} \end{aligned}$$

and

$$\begin{aligned} \beta\hat{\mathbf{f}}_{R^c} - \alpha\nabla^2\hat{\mathbf{f}}_{R^c} &= \beta\mathbf{g} && \text{on } R^c \\ \frac{\partial \hat{\mathbf{f}}_{R^c}}{\partial \vec{\mathcal{N}}} &= 0 && \text{on } \vec{C}. \end{aligned}$$

Over each region of missing data D, the estimation equation reduces to the Laplace equation with the same boundary condition:

$$\begin{aligned} \nabla^2\hat{\mathbf{f}}_D &= 0 && \text{on } D \\ \frac{\partial \hat{\mathbf{f}}_D}{\partial \vec{\mathcal{N}}} &= 0 && \text{on } \vec{C}. \end{aligned}$$

As solutions to the Laplace equation, the estimates obtained over any such missing data regions not containing part of $\vec{C}$ take the form of harmonic functions. As such, we can infer much about the smooth nature of these interpolated estimates as they are subject to both a maximum (and minimum) principle as well as the mean value property. However if the curve $\vec{C}$ intersects D, no such smoothing occurs across this boundary, allowing interpolation to be guided by the segmentation defined by $\vec{C}$. To illustrate this, we show in Figure 2(a) a synthetic image of the US with regions of missing data. The synthetic image is made in an attempt to simulate a satellite picture of the US with regions of incomplete data as a result of obscuration by cloud coverings. The final curve estimate is depicted in Figure 2(d), and the denoise and interpolated reconstruction is shown in Figure 2(e).

Our algorithm can also be used to segment and reconstruct images with isolated pixels of missing data distributed arbitrarily throughout the image. This ability is illustrated in Figure 3 where a forward-looking infrared (FLIR) image of three tanks is shown. The missing data in the FLIR image are due to intensity saturated and defective pixels of the infrared sensor. Using our method, we are able to segment out the tanks and also provide a denoised and complete reconstruction of the image.

4.2. Segmentation-based image magnification

Image magnification capability is weaved into the Mumford-Shah active contour model by considering the image magnification problem as a very structured case of the missing data problem. Specifically, consider a new grid with three times as many pixels in each direction and assign the value of the original image to the "center" pixel in each 3×3 block on the grid and treat the remaining pixels as missing data points. From an estimation-theoretic standpoint, we can view these "center" pixels as sparse measurements on a much larger image domain. We then employ our generalized Mumford-Shah curve evolution procedure to interpolate to this finer grid, using the curve evolution portion of this procedure to partition the domain of the magnified image into different homogeneous subregions so as to provide smooth interpolations where appropriate without blurring across regions of high contrast.

In Figure 4(a), we show a 160×160 noisy black-and-white photograph of 5 burning birthday candles, each of differing intensity. We show in Figure 4(b) the 480×480 magnified image obtained by first magnifying the original noisy image using zero-order hold then smoothing it isotropically. Notice the magnified image is still noisy because the noise components within the original image have been exaggerated by the zero-order interpolation scheme. Figure 4(c) shows the 480×480 magnified image obtained by first isotropically smoothing the original noisy image then magnifying it using zero-order hold. This image is blurry because the edges of the image were destroyed during the initial smoothing step. We show the magnification results based on our approach in Figure 4(d).

5. CONCLUSION

We have described a novel active contour model which brings together the theories of curve evolution, boundary-value stochastic processes, and the Mumford-Shah functional. This model is able to simultaneous segment and smooth images in a single framework and also able to handle problems with missing data. In addition, by extending this model to a segmentation-based approach

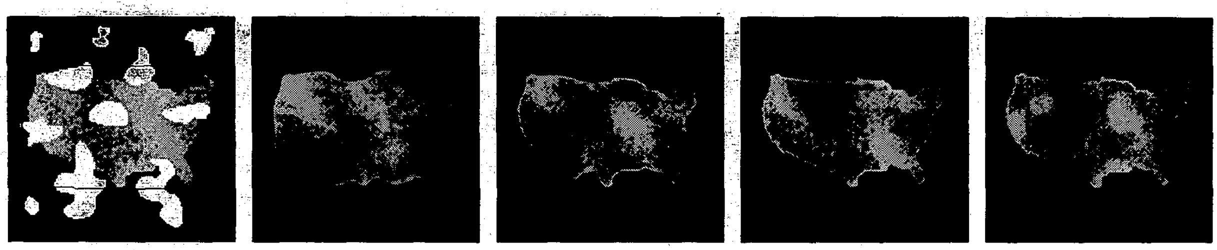

(a) (b) (c) (d) (e)

Fig. 2. Synthetic image with regions of missing data. Missing measurement data points are shown as white pixels in (a).

(a) (b) (c) (d) (e)

Fig. 3. *FLIR image of M2, T62, and M60 tanks. White pixels in (a) denote locations with missing data.*

(a) (b) (c) (d)

Fig. 4. Three-fold magnification of a photograph of birthday candles.

for image magnification, we obtain a magnification technique that is more global, is much less susceptible to blurring or blockiness artifacts as compared to other more traditional techniques, and has the additional attractive denoising capability. In [6], we describe a hierarchical implementation of this model which leads to a fast and efficient algorithm capable of dealing with important image features such as triple points.

6. REFERENCES

[1] M. Adams, A. Willsky, and B. Levy, "Linear estimation of boundary value stochastic processes–part 1: The role and construction of complementary models," *IEEE Trans. Automatic Control*, vol. 29, pp. 803–811, 1984.

[2] T. Chan and L. Vese, "Active contours without edges," UCLA Tech. Report, submitted to *IEEE Trans. Image Processing.*

[3] D. Mumford and J. Shah, "Optimal approximations by piecewise smooth functions and associated variational problems," *Comm. in Pure and Applied Mathematics*, vol. 42, 1989.

[4] S. Osher and J. Sethian, "Fronts propagation with curvature dependent speed: Algorithms based on Hamilton-Jacobi formulations," *Journal of Comp. Phys.*, vol. 79, pp. 12–49, 1988.

[5] N. Paragios and R. Deriche, "Geodesic active regions for texture segmentation," Tech. Report 3440, INRIA, France, 1998.

[6] A. Tsai, A. Yezzi, and A. Willsky, "A Curve Evolution Approach to Smoothing and Segmentation Using the Mumford-Shah Functional" *Proc. IEEE Conf. on Computer Vision and Patt. Recognition*, 2000.

[7] A. Yezzi, A. Tsai, and A. Willsky, "A statistical approach to snakes for bimodal and trimodal imagery" *Int. Conf. on Computer Vision*, 1999.